AGU PUBLICATIONS

Geophysical Research Letters

RESEARCH LETTER
10.1002/2015GL067277

Key Points:
- The natural fracture network is a result of the superposition of multiple tectonic events
- The driving forces for fracturing are released when the fracture network is effectively connected
- The crack-seal cycles can result in an apparent connectivity well above the percolation threshold

Supporting Information:
- Table S1 and Figures S1–S17

Correspondence to:
Q. Lei,
q.lei12@imperial.ac.uk

Citation:
Lei, Q., and X. Wang (2016), Tectonic interpretation of the connectivity of a multiscale fracture system in limestone, *Geophys. Res. Lett.*, *43*, 1551–1558, doi:10.1002/2015GL067277.

Received 2 DEC 2015
Accepted 8 FEB 2016
Accepted article online 10 FEB 2016
Published online 25 FEB 2016

Tectonic interpretation of the connectivity of a multiscale fracture system in limestone

Qinghua Lei[1] and Xiaoguang Wang[1]

[1]Department of Earth Science and Engineering, Imperial College London, London, UK

Abstract This paper studies the statistics and tectonism of a multiscale natural fracture system in limestone. The fracture network exhibits a self-similar characteristic with a correlation between its power law length exponent a and fractal dimension D, i.e., $a \approx D + 1$. Contradicting the scale-invariant connectivity of idealized self-similar systems, the percolation state of trace patterns mapped at different scales and localities of the study area varies significantly, from well to poorly connected. A tectonic interpretation based on a polyphase fracture network evolution history is proposed to explain this discrepancy. We present data to suggest that the driving force for fracture formation may be dissipated at the end of a tectonic event when the system becomes connected. However, the "effective" connectivity can successively be reduced by cementation of early fractures and reestablished by subsequent cracking, rendering a variable "apparent" connectivity that can be significantly above the percolation threshold.

1. Introduction

Fractures ubiquitously exist in crustal rocks and can be classified into three main types based on their kinematic characteristics: opening-mode joints, shear-mode faults, and mixed-mode hybrid fractures [*Pollard and Segall*, 1987]. Fractures form under certain mechanically self-organized dynamics, where breakage and fragmentation can occur at all scales [*Allegre et al*., 1982]. The interaction of fracture growth processes creates a hierarchical geometry that may exhibit long-range correlations from macroscale frameworks to microscale fabrics [*Barton*, 1995; *Bonnet et al*., 2001]. An unresolved debate remains whether natural fractures produced by such critical processes are well or poorly connected [*Berkowitz et al*., 2000].

The geometrical scaling of a fracture population provides clues for a better understanding of the geology and physics behind the statistics. The power law model having no characteristic length scale can be a useful tool to interpret the scaling phenomena of natural fracture systems, which often do not exhibit a representative elementary volume [*Davy*, 1993; *Pickering et al*., 1995; *Odling et al*., 1999; *Marrett et al*., 1999; *Bour et al*., 2002; *Davy et al*., 2010; *Lei et al*., 2015]. In this paper, we first describe the geological setting of a multiscale fracture system in limestone and further analyze its geometrical scaling properties. Based on the knowledge of regional tectonics and a calculation of the percolation parameter of progressively formed fracture networks during multiple tectonic stages, we attempt to interpret an underlying mechanism for the connectivity evolution of the natural fracture system.

2. Geological Setting and Fracture Data Set

The geological formation studied is located in the Languedoc region of SE France and constitutes a major subsurface aquifer (i.e., the Lez aquifer) for the Montpellier area. The aquifer, with a total thickness of ~300 m, is composed of Early Cretaceous marly limestones (upper unit) and Late Jurassic massive limestones (lower unit). The extensive documentation of the tectonic history of this area and good exposure condition of multiscale fracture patterns make such a geological site well suited for the research objective.

The sedimentary basin of SE France contains Mesozoic-Eocene sediments which are characterized by both extensional and compressional tectonic styles [*Séranne et al*., 1995]. A study of the geological evolution of the Languedoc region indicates that this area has been affected by three key tectonic events. The first is the continental stretching related to the Tethyian rifting which occurred in the Jurassic (Event I). This event generated the prevailing normal faults which strike NE-SW across the region [*Benedicto et al*., 1999]. During the Late Cretaceous to Eocene, the stress regime in the area changed from NW-SE extension to N-S compression as a result of the Pyrenean Orogeny. The extensional structures were reactivated as strike-slip faults

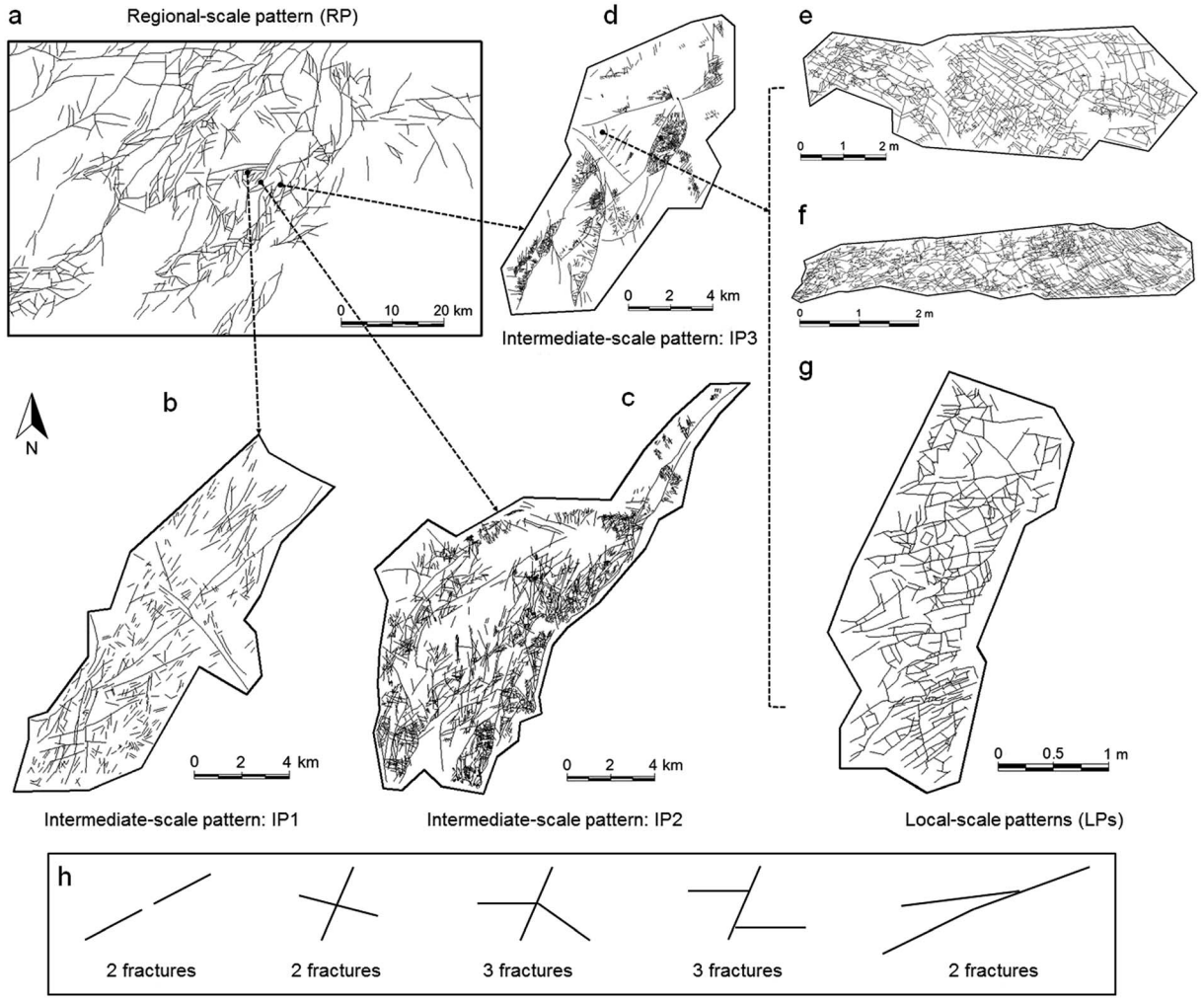

Figure 1. A compilation of multiscale fracture patterns from the Languedoc region in SE France. (a) A regional-scale lineament pattern generated from the regional structural map, (b–d) intermediate-scale fracture patterns obtained from aerial photographs, and (e–g) local-scale outcrop patterns derived from geological exposures. (h) A schematic of the criteria used to distinguish individual fractures from digital maps/images.

during this episode (i.e., Event II-A), which may also have created a strike-slip fault set striking NNW and conjugate to the reactivated Jurassic faults, and an opening-mode joint set aligned along the N-S direction [*Petit and Mattauer*, 1995]. This plate contraction further gave rise to thrusting (Event II-B) and generated thrust faults striking approximately E-W. The crustal extension during the Oligocene (Event III) is related to the opening of the Gulf of Lion and contributed mainly to the rejuvenation of the regional Jurassic normal faults and the creation of a few new minor normal faults [*Benedicto et al*., 1999]. The Lez aquifer experienced intensive rifting, faulting, and folding during the geological history, and consequently a multiscale system of faults and joints has developed as a result of the superposition of multiple fracture sets each linked to a separate tectonic event.

The characterization of the three-dimensional (3-D) structure of the fracture system is impeded by the difficulty of direct measurements, so two-dimensional (2-D) patterns exposed at the Earth's surface are used. A regional-scale (~100 km) fault pattern (Figure 1a), denoted as RP, was generated from the geological map made by *Bureau de Recherches Géologiques et Minières* [2011] at a scale of 1:250,000. Three intermediate-scale (~10 km) fracture patterns containing both faults and joint corridors, denoted as IP1-3 (Figures 1b–1d), were digitized from assembled aerial photographs taken by *Institut National de l'Information Géographique et Forestière* [1954] at a scale of 1:25,000 (resolution may vary slightly due to the uneven terrain). Eleven local-scale (1–10 m) joint patterns, denoted as LPs (three of them are presented in Figures 1e–1g), were drawn based on outcrop mapping. Each

outcrop map was constructed from a number of images taken at a fixed height of 1.5 m and rectified for perspective distortions before assembly. Fractures were manually traced from the digital maps/photographs and individualized according to the spatial continuity and directional consistency of digitized traces (Figure 1h). The determination of the connectedness of fracture traces may be affected by the resolution limits of the original maps/photographs. Some discontinuous segments may be identified as a single fracture, leading to an overestimation of the occurrence of larger structures [*Davy*, 1993]. The fracture patterns may suffer from incomplete sampling producing a bias due to lack of exposure caused by the vegetation covers and erosion effects. This can result in an exaggeration of clustering properties, an underestimation of small-scale populations, and superficial segmentations of large structures. Furthermore, smaller patterns that sample limited local spots of larger domains may underestimate the geological heterogeneity. More details of the multiscale fracture data set are provided in the supporting information.

3. Scaling Properties of the Multiscale Fracture System

The spatial organization and length distribution of fracture networks may be described by a first-order statistical model [*Bour et al.*, 2002]: $n(l, L) = \alpha L^D l^{-a}$, where $n(l, L)dl$ gives the number of fractures with sizes l belonging to the interval $[l, l + dl]$ ($dl << l$) in an elementary volume of characteristic size L, a is the power law length exponent, D is the fractal dimension, and α is the density term. The extent of the power law scaling is bounded by an upper limit l_{max} that is probably related to the thickness of the brittle upper crust and a lower limit l_{min} that is constrained by a physical length scale (e.g., grain size) or the resolution of measurement [*Ouillon et al.*, 1996; *Berkowitz et al.*, 2000]. The exponents a and D quantify different scaling aspects of the fracture network: the length distribution (related to a) and the fracture density (related to D). The density term α is related to the total number of fractures in the system and varies as a function of fracture orientations [*Davy et al.*, 2010].

The fractal dimension D (formally known as the correlation dimension) describes the spatial distribution of fractures. It can be calculated using a two-point correlation function [*Bonnet et al.*, 2001] as defined by $C_2(r) = N_d(r)/N^2$, where N is the total number of fracture barycenters (i.e., midpoint of each fracture trace), and N_d is the number of pairs of barycenters whose separation is smaller than r. For a fractal population, $C_2(r)$ is expected to scale with r following a power law trend, and its exponent gives the value of D. The D value varies for different patterns: 1.68 for RP, 1.66 for IP1, 1.48 for IP2, 1.20 for IP3, and 1.60 ± 0.11 for LPs (the supporting information gives the detailed calculation of D and associated logarithmic slopes for each pattern). The low D values of IP2 and IP3 may be induced by the effects of incomplete sampling, while the variability in LPs is probably related to local stress variations and lithological heterogeneity. Thus, 1.65 might be a realistic value for the underlying fractal dimension, and the fitting trend is shown in Figure 2a.

The power law length exponent a can be derived from the density distribution of fracture lengths [*Pickering et al.*, 1995]. The fracture length data may suffer from the truncation effect due to limited resolution and the censoring effect due to incomplete sampling [*Pickering et al.*, 1995; *Bonnet et al.*, 2001] (the supporting information gives the details of the correction of sampling bias and calculation of a for each pattern). The a value also varies for different patterns: 2.61 for RP, 2.41 for IP1, 2.62 for IP2, 2.53 for IP3, and 2.73 ± 0.38 for LPs. The variation may be influenced by the artifact when tracing individual fractures and determining their persistence, and the bias from incomplete mapping. The large standard deviation in LPs may also be related to the heterogeneity of stress and lithology, to which small-scale fracturing would be more sensitive. Figure 2b gives the length distribution of all fracture networks normalized by their fractal area, i.e., L^D, and the overall trend may be fitted by a power law with $a = 2.65$ and $\alpha = 3.0$.

Fractures having a broad-bandwidth power law size distribution are not randomly placed in the geological media but organized by mechanical interactions that occur during their growth process [*Darcel et al.*, 2003b; *Davy et al.*, 2010, 2013]. The relationship between the fractal dimension and length exponent, i.e., $a \approx D + 1$, indicates that the multiscale fracture system may be self-similar [*Bour et al.*, 2002]. A self-similar fracture pattern is formed under a statistically valid hierarchical rule that a large fracture inhibits smaller ones from crossing it but not the converse [*Davy et al.*, 2010]. The average distance $d(l)$ between the centroid of a fracture and that of the nearest larger neighbor is theoretically correlated with the fracture length l by $d(l) \propto l^x$ [*Bour and Davy*, 1999], where $x = (a - 1)/D$ and is equal to 1.0 for a self-similar scenario. The distance data of the multiscale patterns tend to fit a power law with $x = 1.0$ (Figure 2c), suggesting that the distance of a

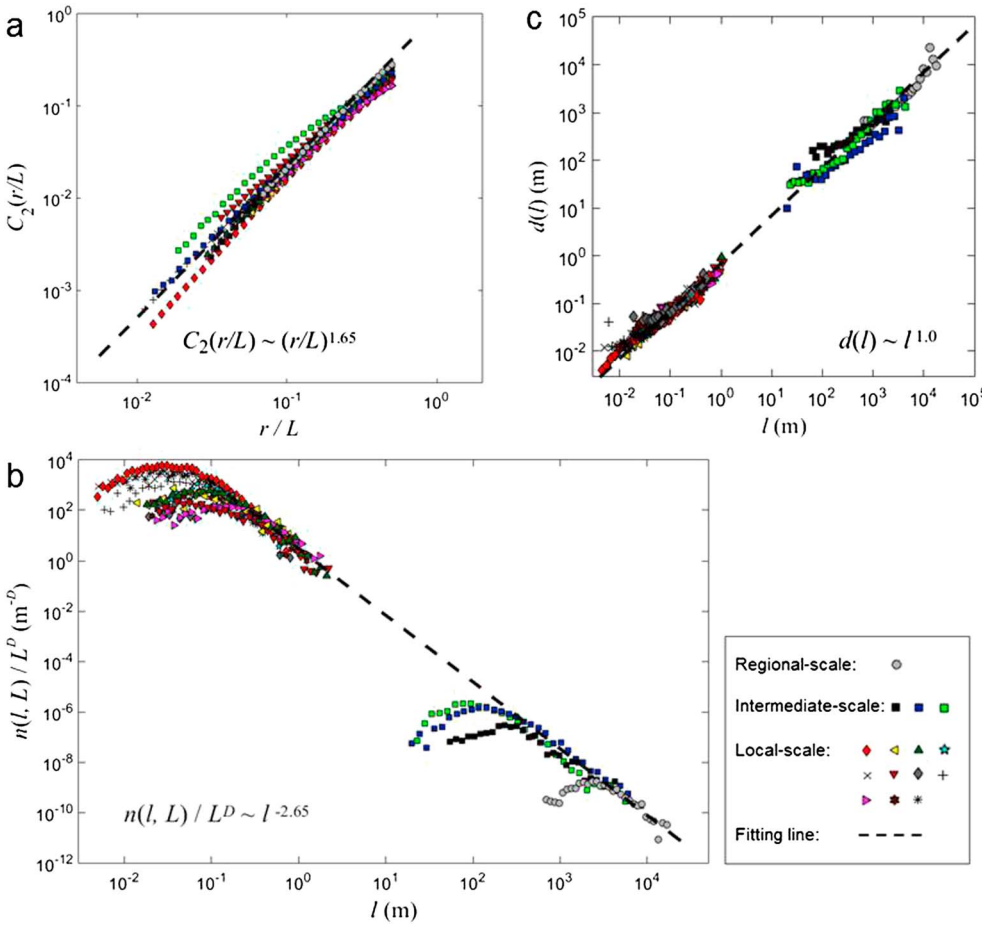

Figure 2. (a) Calculation of the normalized two-point correlation functions $C_2(r/L)$ as a function of r/L. The dashed line represents a power law fitting line with the fractal dimension $D = 1.65$. (b) The normalized density distribution of fracture lengths of the multiscale fracture patterns; the dashed line represents a power law fitting line with an exponent $a = 2.65$ and a density term $\alpha = 3.0$. (c) Scaling of the distance $d(l)$ between the barycenter of a fracture and that of its nearest neighbor having a length larger than l; the dashed line represents a power law fitting line with an exponent $x = 1.0$.

fracture to its nearest larger one is linearly correlated with its size, and that the sets of faults and joints were well developed and had reached quite a dense state controlled by their mechanical interaction [*Davy et al.*, 2010]. In addition, the fracture patterns on different scales also exhibit quite similar values for the ratio of $d(l)/l$, implying that fracture interaction may be governed by a similar mechanism over different scales.

It is complicated to accurately compute the connectivity of a 2-D natural fracture network involving a fractal organization and a power law length distribution [*Darcel et al.*, 2003a]. The complex boundaries of the sampled patterns also create difficulties for a direct connectivity measurement by checking the presence of connected pathways from one boundary to its opposite. We employ a simple equation postulated by *Berkowitz et al.* [2000] to calculate the percolation parameter p as a connectivity metric of fracture networks, as given by

$$p(l, L) = \int_{l_{\min}}^{L} \frac{n(l, L) l^D}{L^D} \mathrm{d}l + \int_{L}^{l_{\max}} n(l, L) \mathrm{d}l \quad (1)$$

Here we define $l_{\min}$ as the fracture length over which all fractures are considered to have been correctly sampled, corresponding to the onset of power law length scaling for each network (given in the supporting information). The connectivity of a fracture network is made up of two parts, as can be seen in equation (1): the first part describes the contribution made by fractures smaller than the system size L and the second represents the contribution from fractures larger than L [*Bour and Davy*, 1997]. Mathematically, the connectivity of a self-similar fractal population is scale invariant [*Darcel et al.*, 2003a], and the networks are connected

Table 1. Percolation Parameters of the Progressively Formed Fracture Patterns at the End of Each Different Formation Stage

Pattern	Stage 1 (Event I)	Stage 2 (Event II-A)	Stage 3 (Events II-B and III)
RP	3.87	5.05	7.18
IP1	3.06	4.30	5.30
IP2	8.16	12.62	14.69
IP3	3.62	5.69	6.90
LPs	--	4.38 ± 1.54	6.81 ± 2.17

at all scales if p is larger than the percolation threshold p_c. Here p_c is defined as the onset above which a fracture network is, on average, connected from one side of the domain to the other. The range of p_c was determined to be between 5.6 and 6.0 derived based on 2-D random fracture network realizations [*Bour and Davy*, 1997]. Uncertainties may exist for this p_c value when being applied to the natural fracture patterns involving distinguishable orientation sets [*Robinson*, 1983, 1984] and fractal density distributions [*Darcel et al*., 2003a]. Furthermore, evaluations relying on this p_c for 2-D networks usually underestimate the connectivity of actual 3-D systems [*Bour and Davy*, 1998]. A correcting factor of $2/\pi$ was suggested to derive a p_c for 3-D geometries [*Lang et al*., 2014], which yields $p_c \approx 3.6$–3.8. In the study area, the p value of the fracture patterns at different scales varies significantly: 7.18 for RP, 5.30 for IP1, 14.69 for IP2, 6.90 for IP3, and 6.81 ± 2.17 for LPs. The computed p should be less than the real value because fractures smaller than l_{min} are not included in the calculation. It can be noted that some patterns seem to be only slightly above the threshold, whereas others have a much higher value. The variation of p may be caused by the diversity of a and D for different samples. The inconsistency in the ratio of L/l_{min} can also have a significant impact on the observed connectivity of a self-similar network [*Berkowitz et al*., 2000]. However, these factors may still not sufficiently explain the high contrast in the calculated p values, i.e., 4.6 to 14.69 (Table S1 in the supporting information).

4. Are Natural Fractures Well or Poorly Connected?

The connectivity of fracture networks is thought to control the bulk properties (e.g., permeability and elastic modulus) of geological formations [*Davy et al*., 2010]. The proximity of the connectivity state of natural fracture networks to the percolation threshold remains an unresolved debate. It was argued earlier that natural fracture systems are close to the percolation threshold [*Renshaw*, 1997], because the driving force (tectonic stress or hydraulic pressure) is abruptly released once the system is connected, and a diminished mechanical strength and an enhanced hydraulic conductivity are likely to occur [*Chelidze*, 1982; *Madden*, 1983; *Gueguen et al*., 1991; *Renshaw*, 1996; *Zhang and Sanderson*, 1998]. However, extensive field observations suggest that crustal fractures can be well connected and significantly above the threshold [*Barton*, 1995].

We propose that an understanding of the process by which the natural fracture networks evolve might offer an explanation for this. Fracture networks in rock develop over geological time by the superposition of successive fracture sets each linked to a different stress regime and set of crustal conditions. Thus, there is a strong possibility that early fracture sets may become partially or totally cemented as the network evolves and fluids move through it. These sealed or partially sealed early fracture sets may act as barriers to fluid flow, and the integrity of the rock has been to some extent recovered [*Holland and Urai*, 2010]. Although the network geometrically remains almost the same, its "effective" connectivity has been reduced well below the percolation threshold. As a result, subsequent stress fields could continue to propagate new fractures until the critical state is reestablished. However, if the "apparent" connectivity of trace patterns is measured without taking into account their internal sealing conditions, it is likely to derive a percolation state significantly above the threshold. In addition, the intrinsic anisotropy of the fracture network may also permit tectonic energy to accumulate in other directions which have a higher mechanical strength/stiffness and can accommodate more new cracks.

To test this concept, we calculate the percolation parameter of the progressively developed fracture networks at the end of each different formation stage (Table 1). The three key tectonic events (see section 2) governed large-scale faulting and jointing and produced the regional-scale and intermediate-scale fracture patterns. These networks are the results of the superimposition of multiple fracture sets; each of which is associated with distinct orientation and linked to a separate tectonic event. The relative ages of the successively generated fracture sets can therefore be determined according to the sequence of the tectonic events [*Park et al*., 2010]. Figure 3 presents a schematic illustration of the kinematic evolution of the studied fracture system during

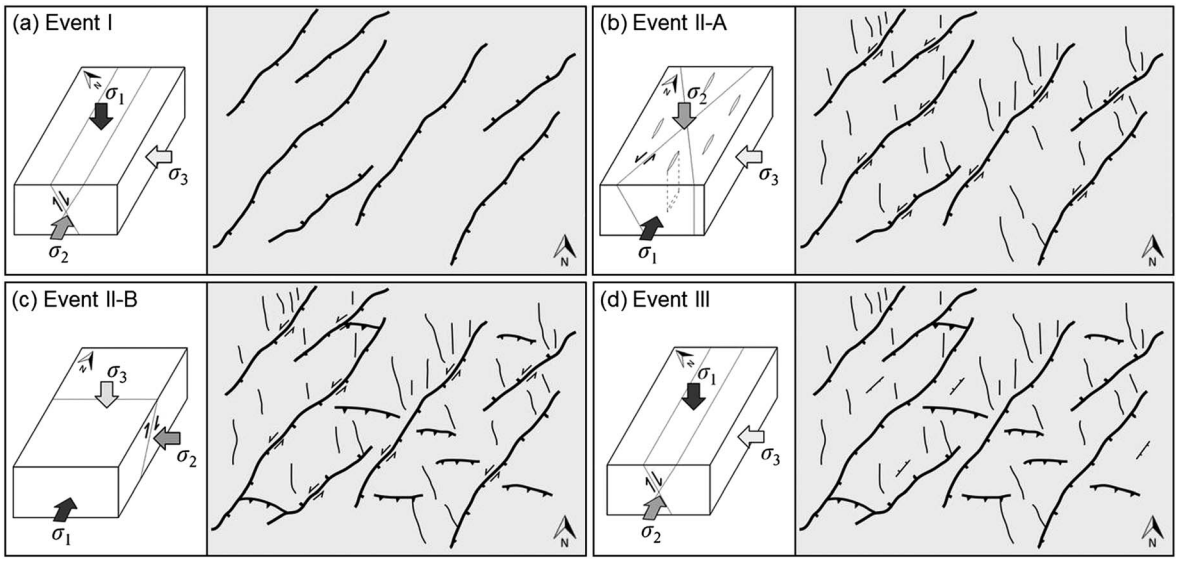

Figure 3. Tectonic events that have affected the geological formations in the Languedoc region, SE France. Note that σ_1, σ_2, and σ_3 denote the maximum, intermediate, and minimum tectonic stresses, respectively.

the tectonic history. At the small scale, e.g., the fracture networks observed in outcrop, the fracture systems are bounded by larger faults and often form close to the ground surface. These larger fractures are likely to severely disturb and rotate the local stress field, and the orientation of the resulting small-scale fractures is, therefore, unlikely to reflect that of the regional stress field. The chronological sequence of the local-scale joints was determined based on the abutting relation of the two major sets. Generally, the first set exhibits a connectivity state close to the percolation threshold (see Table 1), consistent with the postulation of energy relief at the connecting moment observed in both laboratory experiments [*Chelidze*, 1982] and numerical simulations [*Madden*, 1983; *Renshaw*, 1996; *Zhang and Sanderson*, 1998]. However, because of the possibility of early fractures becoming cemented as has been observed in the Languedoc area [*Petit and Mattauer*, 1995; *Petit et al*., 1999], a fracture network which at the time of its formation was at the percolation threshold may subsequently have an effective connectivity considerably lower than p_c. Thus, in response to later tectonic events, further cracking may occur within the network until the system once again becomes connected. The incremental rate of p caused by late-stage fracturing seems to gradually decrease due to the presence of early-stage fractures. This is because percolation can be reached more easily by reactivating and/or coalescing existing fractures rather than by generating new ones. The exceptionally high p in the pattern of IP2 may be attributed to its location very close to one of the regional-scale faults, in the vicinity of which concentrated fracturing paced by active calcite precipitation may occur, i.e., more intensive "crack-seal" cycles may be involved [*Petit and Mattauer*, 1995; *Petit et al*., 1999]. Note that the percolation calculation in this paper seeks to achieve a first-order approximation of the connectivity state that may have existed during the multistage fracture network evolution. The simplified kinematic analysis may not fully capture the complex faulting process that can involve linkage of early-formed fractures in later episodes (i.e., the sizes of large faults may be slightly different from their original ones).

5. Discussion and Conclusions

The evolution of the percolation parameter implies that a large amount of energy may have been released during the early-stage fracturing (as revealed by the high p at the end of the first formation stage of each pattern), after which tectonic or hydraulic forces could not be elevated to such high levels because they would be dissipated by the shearing and coalescence of the existing large structures [*Petit and Mattauer*, 1995; *Park et al*., 2010]. However, relatively small-scale fractures can form during later phases of tectonism [*de Joussineau and Aydin*, 2007; *Park et al*., 2010]. A likely universal scaling behavior may exist in a multiscale fracture system [*Odling et al*., 1999; *Marrett et al*., 1999; *Bour et al*., 2002; *Du Bernard et al*., 2002; *Bertrand et al*., 2015], whereas inconsistent scaling exponents separated by characteristic lengths can also occur [*Ouillon et al*., 1996; *Hunsdale and Sanderson*, 1998; *de Joussineau and Aydin*, 2007; *Putz-Perrier and Sanderson*, 2008; *Davy et al*., 2010]. A break in scaling

may be caused by the different growth mechanisms of jointing and faulting [*Pollard and Segall*, 1987; *de Joussineau and Aydin*, 2007], the influence of lithological layering [*Ouillon et al*., 1996; *Hunsdale and Sanderson*, 1998; *Odling et al*., 1999; *Putz-Perrier and Sanderson*, 2008], and the nature of driving forces (i.e., boundary or body forces) associated with distinct spatial organization of strains [*Bonnet et al*., 2001; *Davy et al*., 2010]. Such effects may have also contributed to the great variability in the scaling exponents of the fracture network in this paper. However, a power law may fit the overall trend of the study system due to a possibility that multiscale fracturing processes in this region were governed by the same set of tectonic factors. The quite low D values (i.e., 1.41–1.74) of the joint patterns in this study, seemingly contradictory to the general understanding that joints tend to be more space filling (i.e., homogeneously distributed), might be induced by the possibility that they have multifractal features; and therefore, the correlation dimension can be significantly smaller than 2.0 [*Bonnet et al*., 2001]. Actually, the measured D values here are in the typical range of 1.4–2.0 for joint systems according to the compilation by *Bonnet et al*. [2001].

In this paper, we proposed an interpretation for the connectivity variation of a multiscale fracture system based on its polyphase tectonic history and a crack-seal mechanism. The results revealed a link between the geometrical statistics of fracture networks and the underlying tectonic processes. Note that the assessment using equation (1) may be associated with uncertainties due to the potential scale dependence of the percolation parameter at the connectivity threshold, as pointed out by *Darcel et al*. [2003a]. Furthermore, the findings of this research are based on a specific fracture system which seems to have a self-similar property with $a \approx D+1$. Different connectivity scaling phenomena can occur in other scenarios [*Darcel et al*., 2003a]. For $a < D+1$, the connectivity, which is controlled by fractures having a length larger than or of the order of the system size, increases with scale. For $a > D+1$, the connectivity is ruled by fractures much smaller than the system size and thus decreases with scale. To investigate the behavior of 3-D fracture systems, the fractal dimension and power law length exponent in 3-D can be extrapolated from the 2-D parameters based on the stereological relationships given in *Darcel et al*. [2003c]. The percolation parameter and percolation threshold of 3-D fracture networks with broadly distributed sizes may be estimated using the formulation proposed by *de Dreuzy et al*. [2000].

To conclude, the spatial and length distributions as well as their cross relation (i.e., fracture distances) of a multiscale fracture system in limestone have been investigated. The connectivity analysis reveals that the percolation state of fracture patterns sampled at different scales and localities of the study area can vary dramatically, from well to poorly connected. The evolution of fracture networks is linked to a succession of tectonic events. For each episode, the tectonic or hydraulic energy available for fracture propagation may be released at the moment when the system reaches the percolation threshold. However, further fracturing may still be accommodated when later driving forces are applied especially if the effective connectivity of the system has been reduced well below the threshold due to the cementation of some of the fractures within the network. As a result, the apparent connectivity measured for fracture networks regardless of their internal sealing conditions can be highly variable and indicate a state considerably exceeding the percolation threshold.

Acknowledgments
We would like to express our sincerest appreciation to John Cosgrove, who contributed substantially to this paper. We thank John-Paul Latham and Lidia Lonergan for their very constructive comments. We also thank David Sanderson, an anonymous referee and the Associate Editor Ake Fagereng for their detailed reviews. We acknowledge Total S.A. for providing financial support and the Janet Watson Scholarship awarded to the first author by the Department of Earth Science and Engineering, Imperial College London. Supporting data are included in the supporting information; any additional data may be obtained from Qinghua Lei (q.lei12@imperial.ac.uk).

References

Allegre, C. J., J. L. Le Mouel, and A. Provost (1982), Scaling rules in rock fracture and possible implications for earthquake prediction, *Nature*, *297*, 47–49, doi:10.1038/297047a0.

Barton, C. C. (1995), Fractal analysis of scaling and spatial clustering of fractures, in *Fractals in the Earth Sciences*, edited by C. C. Barton and P. R. La Pointe, pp. 141–178, Plenum Press, New York.

Benedicto, A., M. Séguret, and P. Labaume (1999), Interaction between faulting, drainage and sedimentation in extensional hanging-wall syncline basins: Example of the Oligocene Matelles basin (Gulf of Lion rifted margin, SE France), in *The Mediterranean Basins: Tertiary Extension Within the Alpine Orogen*, *Geol. Soc. London Spec. Publ*., vol. 156, edited by B. Durand et al., pp. 81–108, Geological Society, London, doi:10.1144/GSL.SP.1999.156.01.06.

Berkowitz, B., O. Bour, P. Davy, and N. Odling (2000), Scaling of fracture connectivity in geological formations, *Geophys. Res. Lett.*, *27*(14), 2061–2064, doi:10.1029/1999GL011241.

Bertrand, L., Y. Géraud, E. Le Garzic, J. Place, M. Diraison, B. Walter, and S. Haffen (2015), A multiscale analysis of a fracture pattern in granite: A case study of the Tamariu granite, Catalunya, Spain, *J. Struct. Geol.*, *78*, 52–66, doi:10.1016/j.jsg.2015.05.013.

Bonnet, E., O. Bour, N. E. Odling, P. Davy, I. Main, P. Cowie, and B. Berkowitz (2001), Scaling of fracture systems in geological media, *Rev. Geophys.*, *39*(3), 347–383, doi:10.1029/1999RG000074.

Bour, O., and P. Davy (1997), Connectivity of random fault networks following a power law fault length distribution, *Water Resour. Res.*, *33*(7), 1567–1583, doi:10.1029/96WR00433.

Bour, O., and P. Davy (1998), On the connectivity of three-dimensional fault networks, *Water Resour. Res.*, *34*(10), 2611–2622, doi:10.1029/98WR01861.

Bour, O., and P. Davy (1999), Clustering and size distribution of fault patterns: Theory and measurements, *Geophys. Res. Lett.*, *26*(13), 2001–2004, doi:10.1029/1999GL900419.

Bour, O., P. Davy, C. Darcel, and N. Odling (2002), A statistical scaling model for fracture network geometry, with validation on a multiscale mapping of a joint network (Hornelen Basin, Norway), *J. Geophys. Res.*, *107*(B6), 2113, doi:10.1029/2001JB000176.
Bureau de Recherches Géologiques et Minières (2011), The geological map of France, scale 1:250,000, Bureau de Recherches Géologiques et Minières, Orléans.
Chelidze, T. L. (1982), Percolation and fracture, *Phys. Earth Planet. Int.*, *28*, 93–101, doi:10.1016/0031-9201(82)90075-9.
Darcel, C., O. Bour, P. Davy, and J.-R. de Dreuzy (2003a), Connectivity properties of two-dimensional fracture networks with stochastic fractal correlation, *Water Resour. Res.*, *39*(10), 1272, doi:10.1029/2002WR001628.
Darcel, C., O. Bour, and P. Davy (2003b), Cross-correlation between length and position in real fracture networks, *Geophys. Res. Lett..*, *30*(12), 1650, doi:10.1029/2003GL017174.
Darcel, C., O. Bour, and P. Davy (2003c), Stereological analysis of fractal fracture networks, *J. Geophys. Res.*, *108*(B9), 2451, doi:10.1029/2002JB002091.
Davy, P. (1993), On the frequency-length distribution of the San Andreas fault system, *J. Geophys. Res.*, *98*, 12,141–12,151, doi:10.1029/93JB00372.
Davy, P., R. Le Goc, C. Darcel, O. Bour, J.-R. de Dreuzy, and R. Munier (2010), A likely universal model of fracture scaling and its consequence for crustal hydromechanics, *J. Geophys. Res.*, *115*, B10411, doi:10.1029/2009JB007043.
Davy, P., R. Le Goc, and C. Darcel (2013), A model of fracture nucleation, growth and arrest, and consequences for fracture density and scaling, *J. Geophys. Res. Solid Earth*, *118*, 1393–1407, doi:10.1002/jgrb.50120.
de Dreuzy, J.-R., P. Davy, and O. Bour (2000), Percolation parameter and percolation-threshold estimates for three-dimensional random ellipses with widely scattered distributions of eccentricity and size, *Phys. Rev. E*, *62*(5), 5948–5952, doi:10.1103/PhysRevE.62.5948.
de Joussineau, G., and A. Aydin (2007), The evolution of the damage zone with fault growth in sandstone and its multiscale characteristics, *J. Geophys. Res.*, *112*, B12401, doi:10.1029/2006JB004711.
Du Bernard, X., P. Labaume, C. Darcel, P. Davy, and O. Bour (2002), Cataclastic slip band distribution in normal fault damage zones, Nubian sandstones, Suez rift, *J. Geophys. Res.*, *107*(B7), 2141, doi:10.1029/2001JB000493.
Gueguen, Y., C. David, and P. Gavrilenko (1991), Percolation networks and fluid transport in the crust, *Geophys. Res. Lett.*, *18*(5), 931–934, doi:10.1029/91GL00951.
Holland, M., and J. L. Urai (2010), Evolution of anastomosing crack-seal vein networks in limestones: Insight from an exhumed high-pressure cell, Jabal Shams, Oman Mountains, *J. Struct. Geol.*, *32*, 1279–1290, doi:10.1016/j.jsg.2009.04.011.
Hunsdale, R., and D. J. Sanderson (1998), Fault distribution analysis—An example from Kimmeridge Bay, Dorset, in *Development, Evolution and Petroleum Geology of the Wessex Basin*, *Geol. Soc. London Spec. Publ.*, vol. 133, edited by J. R. Underhill, pp. 299–310, Geological Society, London, doi:10.1144/GSL.SP.1998.133.01.14.
Institut National de l'Information Géographique et Forestière (1954), Aerial analogic photographs, No. F2543-2843 & F2742-2842, scale 1:25,000, Institut National de l'Information Géographique et Forestière, Paris.
Lang, P. S., A. Paluszny, and R. W. Zimmerman (2014), Permeability tensor of three-dimensional fractured porous rock and a comparison to trace map predictions, *J. Geophys. Res. Solid Earth*, *119*, 6288–6307, doi:10.1002/2014JB011027.
Lei, Q., J.-P. Latham, C.-F. Tsang, J. Xiang, and P. Lang (2015), A new approach to upscaling fracture network models while preserving geostatistical and geomechanical characteristics, *J. Geophys. Res. Solid Earth*, *120*, 4784–4807, doi:10.1002/2014JB011736.
Madden, T. R. (1983), Microcrack connectivity in rocks: A renormalization group approach to the critical phenomena of conduction and failure in crystalline rocks, *J. Geophys. Res.*, *88*(B1), 585–592, doi:10.1029/JB088iB01p00585.
Marrett, R., O. J. Ortega, and C. M. Kelsey (1999), Extent of power-law scaling for natural fractures in rock, *Geology*, *27*(9), 799–802, doi:10.1130/0091-7613.
Odling, N. E., et al. (1999), Variations in fracture system geometry and their implications for fluid flow in fractures hydrocarbon reservoirs, *Pet. Geosci.*, *5*, 373–384, doi:10.1144/petgeo.5.4.373.
Ouillon, G., C. Castaing, and D. Sornette (1996), Hierarchical geometry of faulting, *J. Geophys. Res.*, *101*(B3), 5477–5487, doi:10.1029/95JB02242.
Park, S.-I., Y.-S. Kim, C.-R. Ryoo, and D. J. Sanderson (2010), Fractal analysis of the evolution of a fracture network in a granite outcrop, SE Korea, *Geosci. J.*, *14*(2), 201–215, doi:10.1007/s12303-010-0019-z.
Petit, J.-P., and M. Mattauer (1995), Palaeostress superimposition deduced from mesoscale structures in limestone: The Matelles exposure, Languedoc, France, *J. Struct. Geol.*, *17*(2), 245–256, doi:10.1016/0191-8141(94)E0039-2.
Petit, J.-P., C. A. J. Wibberley, and G. Ruiz (1999), 'Crack-seal', slip: A new fault valve mechanism?, *J. Struct. Geol.*, *21*(8-9), 1199–1207, doi:10.1016/S0191-8141(99)00038-3.
Pickering, G., J. M. Bull, and D. J. Sanderson (1995), Sampling power-law distributions, *Tectonophysics*, *248*(1-2), 1–20, doi:10.1016/0040-1951(95)00030-Q.
Pollard, D. D., and P. Segall (1987), Theoretical displacements and stresses near fractures in rock: With applications to faults, joints, veins, dikes, and solution surfaces, in *Fracture Mechanics of Rock*, edited by B. K. Atkinson, pp. 277–349, Academic Press, San Diego, Calif.
Putz-Perrier, M. A., and D. J. Sanderson (2008), Spatial distribution of brittle strain in layered sequences, *J. Struct. Geol.*, *30*, 50–64, doi:10.1016/j.jsg.2007.10.005.
Renshaw, C. E. (1996), Influence of subcritical fracture growth on the connectivity of fracture networks, *Water Resour. Res.*, *32*(6), 1519–1530, doi:10.1029/96WR00711.
Renshaw, C. E. (1997), Mechanical controls on the spatial density of opening-mode fracture networks, *Geology*, *25*(10), 923–926, doi:10.1130/0091-7613(1997)025<0923:MCOTSD>2.3.CO;2.
Robinson, P. C. (1983), Connectivity of fractures systems—A percolation theory approach, *J. Phys. A*, *16*, 605–614, doi:10.1088/0305-4470/16/3/020.
Robinson, P. C. (1984), Numerical calculations of critical densities for lines and planes, *J. Phys. A*, *17*, 2823–2830, doi:10.1088/0305-4470/17/14/025.
Séranne, M., A. Benedicto, P. Labaum, C. Truffert, and G. Pascal (1995), Structural style and evolution of the Gulf of Lion Oligo-Miocene rifting: Role of the Pyrenean orogeny, *Mar. Pet. Geol.*, *12*(8), 809–820, doi:10.1016/0264-8172(95)98849-Z.
Zhang, X., and D. J. Sanderson (1998), Numerical study of critical behaviour of deformation and permeability of fractured rock masses, *Mar. Pet. Geol.*, *15*(6), 535–548, doi:10.1016/S0264-8172(98)00030-0.